

## Generalized oscillator strength of the core-excited states of molecular nitrogen studied by nonresonant inelastic x-ray scattering

Li-Han Wang,<sup>1</sup> Tao Xiong,<sup>2,3</sup> Xu Kang,<sup>4</sup> Zhi-Wei Nie,<sup>1</sup> Jin-Feng Chen,<sup>1</sup> Zhen Xie,<sup>1</sup> Shuai Yan,<sup>5</sup> Ai-Guo Li,<sup>5</sup> Yuan-Chen Xu,<sup>1</sup> Shu-Xing Wang<sup>1</sup>,<sup>\*</sup> Ke Yang,<sup>5,\*</sup> and Lin-Fan Zhu<sup>1,†</sup>

<sup>1</sup>Hefei National Research Center for Physical Sciences at Microscale and Department of Modern Physics, University of Science and Technology of China, Hefei, Anhui 230026, People's Republic of China

<sup>2</sup>Institute of High Energy Physics, Chinese Academy of Sciences (CAS), Beijing 100049, People's Republic of China

<sup>3</sup>Spallation Neutron Source Science Center (SNSSC), Dongguan 523803, People's Republic of China

<sup>4</sup>Institute of Fluid Physics, China Academy of Engineering Physics, Mianyang, Sichuan 621900, People's Republic of China

<sup>5</sup>Shanghai Advanced Research Institute, Chinese Academy of Sciences, Shanghai 201210, People's Republic of China



(Received 19 May 2022; accepted 29 July 2022; published 11 August 2022)

Fast electron impact was used to study the generalized oscillator strengths of the inner-shell excitations in atoms and molecules previously. In this work, a nonresonant inelastic x-ray scattering technique is extended to determine the generalized oscillator strengths of  $(1\sigma_g \rightarrow 1\pi_g) + (1\sigma_u \rightarrow 1\pi_g)$  inner-shell excitations of molecular nitrogen in the squared momentum transfer range of 0.86 to 14.40 a.u. at a photon energy of about 10 keV and an energy resolution of about 1.3 eV. The present generalized oscillator strength strictly follows the first Born approximation and thus provides a rigorous test to the previously calculated results and the experimental ones measured by the electron energy loss spectroscopy. The presently extrapolated optical oscillator strength at zero momentum transfer is in accord with most experimental results and the theoretical data with the correlation effect considered carefully. This work indicates that the nonresonant inelastic x-ray scattering technique is a powerful tool to study the core excitation mechanism in atoms and molecules.

DOI: [10.1103/PhysRevA.106.022806](https://doi.org/10.1103/PhysRevA.106.022806)

### I. INTRODUCTION

Core excitation is a unique characteristic of elements and attracts widespread attention. Generally, the core excited states of atoms or molecules were studied by x-ray photoabsorption spectroscopy, and the dynamical processes were explored by the resonant inelastic x-ray scattering (RIXS) and resonant Auger spectroscopy (RAS) techniques. From these dynamical processes, many phenomena [1–3], such as the spatial quantum beats and the collapse of vibrational structure, were observed and the potential energy surfaces were extracted [4,5]. The core-hole created in the inner-shell excitation of the molecule with inversion symmetry encounters the well-known localization puzzle, i.e., whether the created core-hole is localized around a single atom or delocalized over different ones. For the homonuclear diatomic molecule such as  $N_2$ , the localization picture predicts one final states for the  $1s$  ionization or excitation, while the delocalization picture predicts two final states due to the  $g-u$  splitting of  $1s$  core holes. Furthermore, the localization or delocalization picture also presents the asymmetric or symmetric angular distribution of the photoelectrons, Auger electrons, and ionic fragments. As a result different experimental techniques including photoelectron, Auger electron, ionic fragment spectroscopies, as well as the coincidence one were used to explore

this issue [6–9]. More recently, the  $1s$  core hole created in the excitation of  $N_2$  was studied by using a high-resolution angle-resolved electron energy loss spectrometer [10]. In addition, the relaxation [11] and electron correlation effects accompanied with the core excitation further complicated theoretical studies. Usually, these effects could be tested by comparing the experimental results with the theoretical calculations, with and without the corresponding corrections [12].

In addition to the excitation energy, the generalized and optical oscillator strengths can also be used to test the calculated wave functions of the inner-shell excited states. Photoabsorption measurements were widely used to determine the excitation energy and corresponding optical oscillator strength (OOS). The generalized oscillator strength (GOS) was first introduced by Bethe [13,14] to describe the collisional excitation by charged particles in atoms and molecules. For a definite transition at the excitation energy  $E_n$ , the GOS is defined as [15,16]

$$f(\mathbf{K}, E_n) = \frac{2E_n}{K^2} \frac{1}{4\pi} \int \zeta(\mathbf{K}, E_n) d\Omega, \quad (1)$$

with

$$\zeta(\mathbf{K}, E_n) = \left| \left\langle \Psi_n \left| \sum_{j=1}^N \exp(i\mathbf{K} \cdot \mathbf{r}_j) \right| \Psi_0 \right\rangle \right|^2. \quad (2)$$

Here,  $f(\mathbf{K}, E_n)$  stands for the GOS, and  $\zeta(\mathbf{K}, E_n)$  is the inelastic squared form factor (ISFF).  $\Psi_0$  and  $\Psi_n$  are the  $N$ -electron wave functions for the initial and final states, respectively.  $\mathbf{K}$

\*yangke@zjlab.org.cn

†lfzhu@ustc.edu.cn

is the momentum transfer vector from the the charged particle or x ray to the target and  $K$  is the norm of the vector  $\mathbf{K}$ .  $\mathbf{r}_j$  is the position vector of the  $j$ th electron. The integration of  $\Omega$  represents the average over the orientation of the molecular axis with respect to  $\mathbf{K}$ . The momentum transfer dependence behavior of GOS provides fresh insight into the theoretically calculated wave functions of inner-shell excited states. A fast electron was commonly used to probe the GOS for atoms and molecules previously by using an angle-resolved electron energy loss spectrometer. Usually, the first Born approximation (FBA) works well for low-lying valence excited states when the incident electron energy approaches several keV [15,16]. However, the core excitation energy usually reaches several hundreds eV, making it difficult to satisfy the FBA by increasing the incident electron energy. In addition, many difficulties are brought about by the small scattering cross sections and the complicated normalization procedure. Therefore, the experiments for core excitation GOSs are much less than those of valance ones [17].

Nonresonant inelastic x-ray scattering (NRIXS) technique was already used to measure the GOSs of low-lying valence excited states in atoms and molecules since 2010 [18,19], and has also been used to study vibronic effects in the x-ray absorption near the edge structure of  $\text{N}_2$ ,  $\text{N}_2\text{O}$ , and  $\text{CO}_2$  molecules [20]. When the energy of the incident photon is far away from the resonance, the relationship between the GOS and the x-ray scattering cross section can be described as

$$f(K, E_n) = \frac{1}{r_0^2} \frac{2E_n}{K^2} \frac{\omega_i}{\omega_f} \frac{1}{|\boldsymbol{\varepsilon}_i \cdot \boldsymbol{\varepsilon}_f^*|^2} \left( \frac{d\sigma}{d\Omega} \right)_\gamma. \quad (3)$$

Here,  $\left( \frac{d\sigma}{d\Omega} \right)_\gamma$  stands for the x-ray scattering cross section,  $\omega_i$  and  $\omega_f$  are the energies of the incident and scattered photons, and  $r_0 \equiv e^2/m_e c^2$  is the classical electron radius.  $\boldsymbol{\varepsilon}_i$  and  $\boldsymbol{\varepsilon}_f$  are the polarized vectors of the incident and scattered photons, and  $|\boldsymbol{\varepsilon}_i \cdot \boldsymbol{\varepsilon}_f^*|^2$  equals 1 if the polarization directions of the photons are perpendicular to the scattering plane, which is the adopted arrangement of this work. The major advantages of x-ray scattering are as follows [21]: (1) The form of the NRIXS transition matrix element is equal to the FBA satisfied electron energy loss spectroscopy (EELS) one, while the validity condition in the electron impact method is a complex and difficult problem [22,23]; (2) the scattering cross sections do not decrease according to the law of  $1/K^4$  as in the EELS method when the momentum transfer increases [24]; and (3) the normalization procedure is very simple. To date, NRIXS has not been used to determine absolute GOS data for core excited states in atoms and molecules. Here, we extend its application for measuring the GOS of the  $(1\sigma_g \rightarrow 1\pi_g) + (1\sigma_u \rightarrow 1\pi_g)$  core excitation in molecular nitrogen ( $\text{N}_2$ ).

The GOSs for the  $(1\sigma_g \rightarrow 1\pi_g) + (1\sigma_u \rightarrow 1\pi_g)$  core excitations in  $\text{N}_2$  were studied both experimentally (electron scattering) and theoretically [25–29]. Experimentally, the measured GOSs are highly correlated to the incident electron energy. The recent study on the core excitation in  $\text{N}_2$  [10] by the high-resolution EELS focused on resolving the dipole-allowed and dipole-forbidden transition components. However, the incident electron energy of 1500 eV was far from satisfying the FBA, and the absolute GOS for the core excitations were not available in their work. The FBA seems

to be satisfied when the incident electron energy is as high as 25 keV because the experimental results are very close to the GMSCI-calculated results [26,28]. However, it is still necessary to use another completely different method to cross check it. Therefore, in the present work, the absolute GOS for the  $(1\sigma_g \rightarrow 1\pi_g) + (1\sigma_u \rightarrow 1\pi_g)$  core excitation in  $\text{N}_2$  is measured by using x-ray scattering, demonstrating the feasibility of NRIXS in determining GOSs for core excitations of atoms and molecules.

## II. EXPERIMENTAL METHODS

The experiment was carried out at the beamline BL15U at Shanghai Synchrotron Radiation Facility (SSRF). A detailed description of the instrument can be found in Ref. [30], and the measurement was performed at incident photon energies around 9885.7 and 10286 eV with an energy resolution of about 1.3 eV to measure the elastic and inelastic scattered signals, respectively. During the measurement, the Si(555) spherical crystal photon analyzer was operated at a fixed energy of 9885.7 eV. The energy loss spectra were collected by scanning the incident photon energy. The squared momentum transfers from 0.86 to 14.40 a.u. were realized by varying the scattering angles from  $20^\circ$  to  $90^\circ$ . Considering the small excitation cross section, the  $\text{N}_2$  gas was compressed in a chamber sealed by the beryllium window at a pressure of 10 atm to increase the scattering intensity. The incoming and outgoing photon paths were filled with helium gas to avoid strong absorption by the air.

Absolute GOS data were obtained by normalizing the inelastic scattering intensity to the elastic scattering signals measured at the same angle via

$$f(K, E_n) = \frac{2E_n}{K^2} \frac{\omega_{\text{inel}}}{\omega_{\text{el}}} \frac{N_{\text{inel}}(E_n, \theta)}{N_{\text{el}}(\theta)} \frac{1}{4\pi} \int \zeta(\mathbf{K}) d\Omega. \quad (4)$$

Here,  $N_{\text{inel}}$  and  $N_{\text{el}}$  are inelastic and elastic scattering intensities that are normalized to the photon flux monitored in real time.  $\omega_{\text{inel}}$  and  $\omega_{\text{el}}$  are the energies of the incident photons for the measurements of inelastic and elastic signals, respectively.  $\theta$  is the scattering angle. The gas pressure and the effective interaction length are eliminated since they are identical for the inelastic and elastic scatterings. The elastic squared form factor (ESFF)  $\zeta(\mathbf{K})$  is defined as

$$\zeta(\mathbf{K}) = \left\langle \left| \Psi_0 \left| \sum_{j=1}^N \exp(i\mathbf{K} \cdot \mathbf{r}_j) \right| \Psi_0 \right| \right\rangle^2. \quad (5)$$

The ESFF of  $\text{N}_2$  are calculated with the theoretical ground-state wave function prepared by the GAUSSIAN16 program using density functional theory (DFT-B3LYP) with the aug-cc-pVTZ basis set [31–33]. Note that the core excitation signals are actually superimposed on the Compton profile and the stray photons constitute the background. To extract the absolute inelastic scattering intensities for core excitation, the Compton profile was also calculated with the ground-state wave function. The Compton profile and the calculated GOS by Bielschowsky *et al.* [28] are used to calculate the x-ray scattering intensities. Figure 1(a) presents the simulated NRIXS spectrum by convoluting the calculations with the present instrumental function at  $30^\circ$ . As shown in Fig. 1(b),

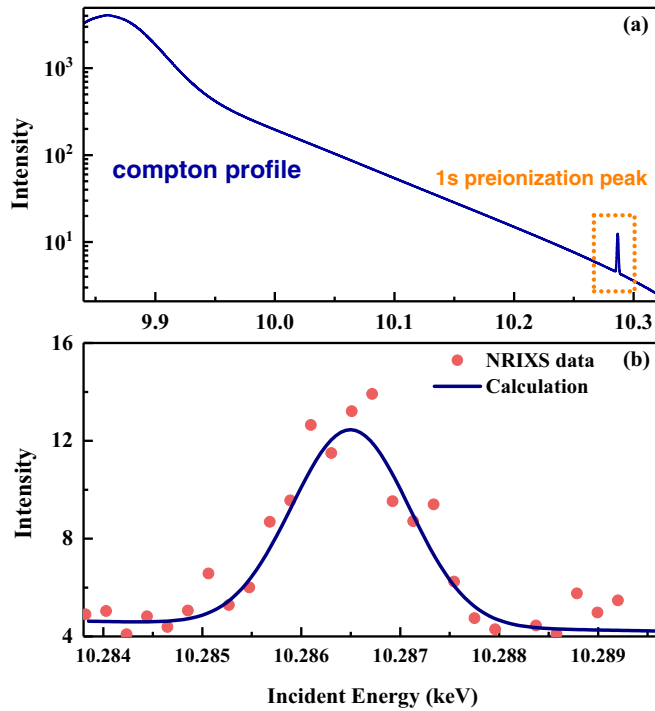


FIG. 1. (a) The calculated NRIXS spectrum at  $30^\circ$ . (b) The comparison of the present experimental data and calculated results between 10.284 keV and 10.289 keV.

the simulated spectrum is in fair agreement with the experimental data. The background signals could be subtracted with a linear function in the least-squares fitting since the line width of the core excitation is quite narrow compared to the width of the Compton profile.

Since the instrumental function cannot be described by a single Gaussian function [30], we use three Gaussian functions to fit the elastic peak as shown in Fig. 2(a), and take it as the instrumental function. An additional Gaussian profile accounting for the broadening effect of core excitation is convoluted with the instrumental function to fit the core excitation spectra [21]. Figure 2(b) shows the inelastic core excitation spectrum at  $30^\circ$  and the fitted curve. The excitation energy is determined as 401.1 eV.

The experimental error of the present GOS includes the contributions from the finite angular resolution, the angle determination, the statistical counts, the least-squares fitting, and the normalizing procedure. The total experimental errors are generally around 10–15% as shown in the corresponding figures.

### III. RESULTS AND DISCUSSION

$N_2$  is a molecule with the ground-state configuration of  $1\sigma_g^2 1\sigma_u^2 2\sigma_g^2 2\sigma_u^2 1\pi_u^4 3\sigma_g^2 1\pi_g^0 3\sigma_u^0$ . In this work we describe the excited states in the delocalized frame, i.e., the core excitation does not break the symmetry and the excitation feature at around 401.1 eV consists of the dipole-forbidden  $1\sigma_g \rightarrow 1\pi_g$  and the dipole-allowed  $1\sigma_u \rightarrow 1\pi_g$  components. The energy interval between these two states is 67 meV [10,27,28,34,35], which is much narrower than the present energy resolution

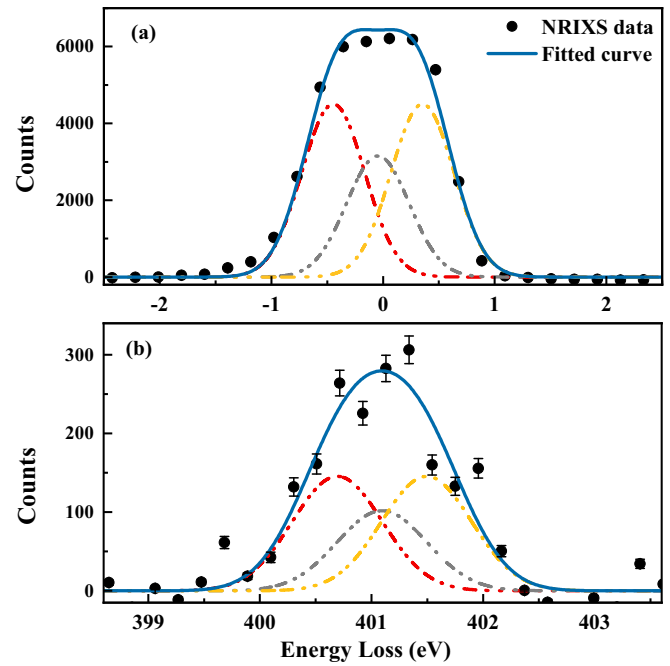


FIG. 2. The present data and fitted results at  $30^\circ$  for (a) the elastic peak and (b) the 1s preionization peak.

of 1.3 eV. Therefore, the sum GOS of these two states is determined in the present work.

Figure 3 shows the comparisons of the present GOS with the previous experimental [25,26] and theoretical [27–29] data. The EELS measurement at 3.4 keV is generally lower than the present x-ray scattering data and the calculations except the data in  $K^2 \leq 1$  a.u., which may be caused by the failure of the FBA. At high electron energy of 25 keV [26], the EELS data agree better with the x-ray scattering and FBA calculated results. The oscillatory GOS data with respect to  $K^2$  and the slightly lower values in  $K^2 \leq 1$  a.u. at 25 keV are likely to be attributed to the limited angu-

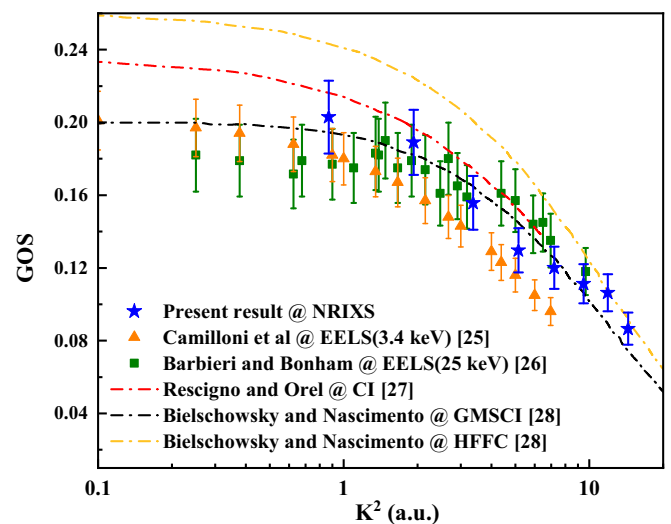


FIG. 3. The sum GOS of  $1\sigma_g \rightarrow 1\pi_g$  and  $1\sigma_u \rightarrow 1\pi_g$  along with the previous experimental and theoretical results for comparison.

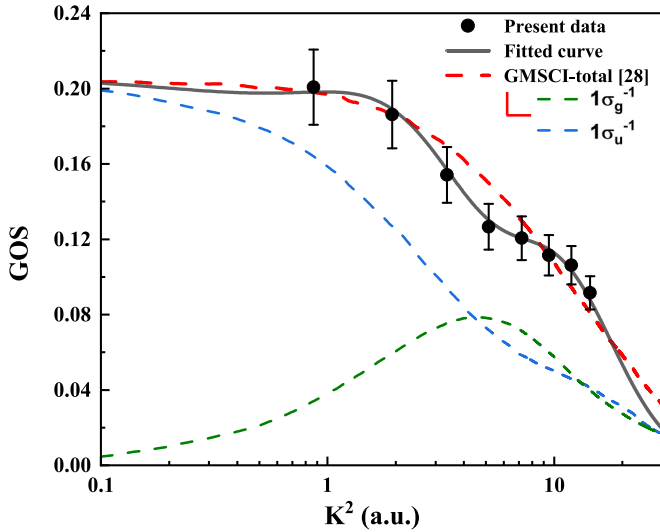


FIG. 4. Comparison between the present GOS of ( $1\sigma_g \rightarrow 1\pi_g$ ) + ( $1\sigma_u \rightarrow 1\pi_g$ ) and the calculated results in Ref. [28]. The green and blue dashed curves represent the separate GOS of these two transitions. The red curve is the sum GOS of these two transitions and the gray line represents the result fitted by the Lassetre formula [36].

lar resolution and the difficulty in angle determination at a very high incident electron energy. Rescigno and Orel [27] calculated the GOS for the core excitation in  $N_2$  using the limited configuration-interaction (CI) calculations with localized  $1\sigma$  orbitals. Theoretical results were also obtained by the Hartree-Fock frozen-core calculation (HFFC) and by using a generalized multistructural wave function in a nonorthogonal configuration interaction (GMSCI) approach [28]. The HFFC data, which do not include the relaxation, localization, and correlation effects, are prominently higher than the electron impact and x-ray scattering data. The GMSCI calculation, incorporating all the important effects necessary to describe the core excited state, yields a fair agreement with the present measurement. More recently, the core excitation in  $N_2$  has also been studied by the distorted-wave approximation [29].

Moreover, a shoulder structure around  $K^2 = 8$  a.u. is observed in the present x-ray scattering data. As shown in Fig. 4, the shoulder structure could be caused by the overlap of the dipole-allowed ( $1\sigma_u \rightarrow 1\pi_g$ ) and dipole-forbidden ( $1\sigma_g \rightarrow 1\pi_g$ ) components. Note that the GOS for a dipole-allowed transition has a maximum at  $K^2 = 0$  a.u. and decreasing with increasing  $K^2$ , while the GOS for a dipole-forbidden transition has a maximum at nonzero  $K^2$ . The calculated GOS profiles show no evidence of shoulder structure. In all probability, the calculated maximum GOS for the ( $1\sigma_g \rightarrow 1\pi_g$ ) transition, which is very sensitive to the accuracy of the wave functions, is shifted to lower  $K^2$ . The shifted maximum GOS of dipole-forbidden transition was also observed in the valence-shell excitations [37,38]. In addition, the present extracted excitation energy of 401.1 eV is consistent with the calculated data by Bielschowsky *et al.* [28] with localized orbitals. However, the calculation with delocalized orbitals yielded a 9 eV shift to higher energy, indicating that the correlation effect can be

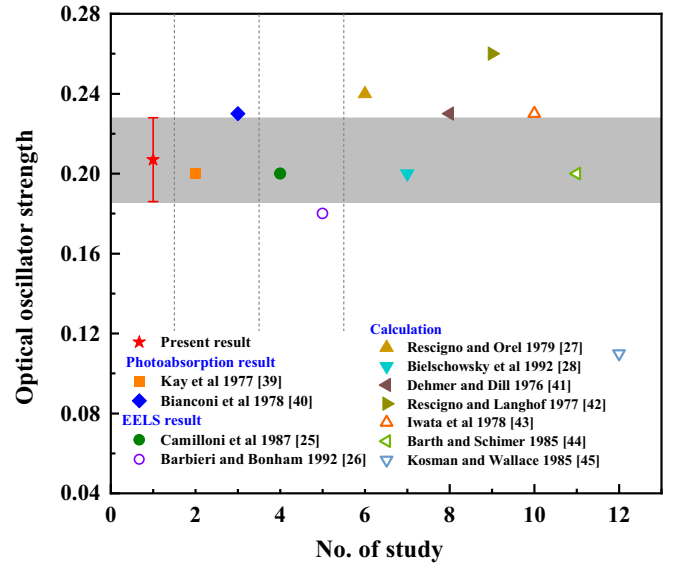


FIG. 5. Present OOS of  $1\sigma_u \rightarrow 1\pi_g$  along with the previous available experimental and theoretical ones.

effectively compensated by including the localized orbitals as mentioned in Ref. [6].

Using the Lassetre formula [36], the experimental GOS is extrapolated to  $K^2 = 0$  a.u., getting the OOS for the  $1\sigma_u \rightarrow 1\pi_g$  transition. The extrapolated OOS of 0.198 provides an independent cross check to previous experimental [25,26,39,40] and theoretical [27,28,41–45] results, as shown in Fig. 5. The extrapolation agrees with the photoabsorption measurement by Kay *et al.* [39] and the EELS results by Camilloni *et al.* [25] and Barbieri and Bonham [26]. The photoabsorption measurement by Ref. [40] is higher than the present extrapolation beyond the error bar. Note that the correlation effect was not considered seriously in most of the theoretical works and the calculated data differ from the present data. The calculations by Bielschowsky *et al.* [28] and Barth and Schirmer [44] agree with the present data since the correlation effect was included. The former authors incorporated the correlation by using localized orbitals while the latter authors included three electron excitation contribution in the configuration space. In general, the correlation effect is crucial for obtaining an accurate oscillator strength of the core excitations.

#### IV. CONCLUSION

In summary, the nonresonant inelastic x-ray scattering method was extended to measure the generalized oscillator strength for core excitation. The sum GOS of the  $1\sigma_g \rightarrow 1\pi_g$  and  $1\sigma_u \rightarrow 1\pi_g$  transitions in  $N_2$  is determined. The measured GOS generally agrees with the high-energy EELS measurement and the calculations under the FBA. Moreover, the measured GOS is extrapolated to  $K^2 = 0$  a.u. to determine the optical oscillator strength for the dipole-allowed  $1\sigma_u \rightarrow 1\pi_g$  transition. The extrapolation agrees well with most photoabsorption and electron impact measurements. Further comparisons between the experimental data and theoretical calculations indicate that the correlation effect is crucial in obtaining an accurate oscillator strength for core

excitation. The present work indicates that the NRIXS is a powerful tool to provide reliable inner-shell GOS and OOS data for molecules. The obtained data can be used to test the theoretical wave functions strictly.

The implementation of the FBA in EELS studies has been a complex problem since the validity condition depends not only on the transition types for a definite target, but also on the momentum transfers. The convergent behavior of the measured GOS with increasing incident electron energy was usually regarded as a criterion for the FBA in the EELS experiment, while the convergence does not always indicate that the FBA is feasible [38]. Nevertheless, the GOS determined by the NRIXS method is identical to the data within the framework of the FBA, which can serve as an independent

cross check to the EELS measurements. The rapid progress of synchrotron radiation, x-ray free electron laser, and multi-channel analyzer would offer great opportunities for the GOS measurements of core excitations by using the NRIXS technique with high-energy resolution and good statistical counts [46,47].

## ACKNOWLEDGMENTS

This work was partially supported by the National Natural Science Foundation of China (Grants No. U1932207 and No. 12104437) and the Guangdong Basic and Applied Basic Research Foundation (Grant No. 2021A1515111164).

- 
- [1] A. Pietzsch, Y. P. Sun, F. Hennies, Z. Rinkevicius, H. O. Karlsson, T. Schmitt, V. N. Strocov, J. Andersson, B. Kennedy, J. Schlappa, A. Fohlisch, J. E. Rubensson, and F. Gel'mukhanov, *Phys. Rev. Lett.* **106**, 153004 (2011).
- [2] V. Vaz da Cruz, N. Ignatova, R. C. Couto, D. A. Fedotov, D. R. Rehn, V. Savchenko, P. Norman, H. Ågren, S. Polyutov, J. Niskanen *et al.*, *J. Chem. Phys.* **150**, 234301 (2019).
- [3] M. N. Piancastelli, T. Marchenko, R. Guillemin, L. Journal, O. Travnikova, I. Ismail, and M. Simon, *Rep. Prog. Phys.* **83**, 016401 (2020).
- [4] T. Marchenko, G. Goldsztejn, K. Jänkälä, O. Travnikova, L. Journal, R. Guillemin, N. Sisourat, D. Céolin, M. Žitnik, M. Kavčič *et al.*, *Phys. Rev. Lett.* **119**, 133001 (2017).
- [5] S. Eckert, V. V. da Cruz, F. Gel'mukhanov, E. Ertan, N. Ignatova, S. Polyutov, R. C. Couto, M. Fondell, M. Dantz, B. Kennedy *et al.*, *Phys. Rev. A* **97**, 053410 (2018).
- [6] L. Cederbaum and W. Domcke, *J. Chem. Phys.* **66**, 5084 (1977).
- [7] O. Bjorneholm, M. Bassler, A. Ausmees, I. Hjelte, R. Feifel, H. Wang, C. Miron, M. N. Piancastelli, S. Svensson, S. L. Sorensen, F. Gel'mukhanov, and H. Agren, *Phys. Rev. Lett.* **84**, 2826 (2000).
- [8] J. I. Adachi, K. Hosaka, T. Teramoto, M. Yamazaki, N. Watanabe, M. Takahashi, and A. Yagishita, *J. Phys. B: At., Mol. Opt. Phys.* **40**, F285 (2007).
- [9] M. S. Schoffler, J. Titze, N. Petridis, T. Jahnke, K. Cole, L. P. H. Schmidt, A. Czasch, D. Akoury, O. Jagutzki, J. Williams *et al.*, *Science* **320**, 920 (2008).
- [10] Y.-C. Xu, S.-X. Wang, X.-J. Du, L.-H. Wang, and L.-F. Zhu, *New J. Phys.* **24**, 053036 (2022).
- [11] O. Takahashi, N. Kunitake, and S. Takaki, *J. Phys. B: At., Mol. Opt. Phys.* **48**, 204001 (2015).
- [12] C. E. V. de Moura, R. R. Oliveira, and A. B. Rocha, *J. Mol. Model.* **19**, 2027 (2013).
- [13] H. Bethe, *Ann. Phys. (Leipzig)* **397**, 325 (1930).
- [14] H. Bethe, *Z. Phys.* **76**, 293 (1932).
- [15] M. Inokuti, *Rev. Mod. Phys.* **43**, 297 (1971).
- [16] J. Sakurai and J. Napolitano, *Modern Quantum Mechanics*, 2nd ed., (Pearson, New York, 2014).
- [17] A. P. Hitchcock, *J. Electron Spectrosc. Relat. Phenom.* **112**, 9 (2000).
- [18] B. P. Xie, L. F. Zhu, K. Yang, B. Zhou, N. Hiraoka, Y. Q. Cai, Y. Yao, C. Q. Wu, E. L. Wang, and D. L. Feng, *Phys. Rev. A* **82**, 032501 (2010).
- [19] L. F. Zhu, L. S. Wang, B. P. Xie, K. Yang, N. Hiraoka, Y. Q. Cai, and D. L. Feng, *J. Phys. B: At., Mol. Opt. Phys.* **44**, 025203 (2011).
- [20] A. Sakko, S. Galambosi, J. Inkinen, T. Pylkkänen, M. Hakala, S. Huotari, and K. Hämäläinen, *Phys. Chem. Chem. Phys.* **13**, 11678 (2011).
- [21] W. Schülke, *Electron Dynamics by Inelastic X-Ray Scattering* (Oxford University Press, New York, 2007).
- [22] M. Blume, *J. Appl. Phys.* **57**, 3615 (1985).
- [23] L. F. Zhu, W. Q. Xu, K. Yang, Z. Jiang, X. Kang, B. P. Xie, D. L. Feng, N. Hiraoka, and K. D. Tsuei, *Phys. Rev. A* **85**, 030501(R) (2012).
- [24] S. X. Wang and L. F. Zhu, *Matter Radiat. Extremes* **5**, 054201 (2020).
- [25] R. Camilloni, E. Fainelli, G. Petrocelli, and G. Stefani, *J. Phys. B: At. Mol. Phys.* **20**, 1839 (1987).
- [26] R. S. Barbieri and R. A. Bonham, *Phys. Rev. A* **45**, 7929 (1992).
- [27] T. N. Rescigno and A. E. Orel, *J. Chem. Phys.* **70**, 3390 (1979).
- [28] C. E. Bielschowsky, M. A. C. Nascimento, and E. Hollauer, *Phys. Rev. A* **45**, 7942 (1992).
- [29] S. E. Michelin, A. de Campos, L. S. S. da Silva, A. S. Falck, E. A. y Castro, O. Pessoa, H. L. Oliveira, and M. T. Lee, *Chem. Phys.* **293**, 365 (2003).
- [30] D. D. Ni, X. Kang, S. Yan, X. C. Huang, T. Xiong, D. X. Liang, K. Yang, and L. F. Zhu, *Rev. Sci. Instrum.* **89**, 085108 (2018).
- [31] M. J. Frisch, G. W. Trucks, H. B. Schlegel, G. E. Scuseria, M. A. Robb, J. R. Cheeseman, G. Scalmani, V. Barone, G. A. Petersson, H. Nakatsuji *et al.*, GAUSSIAN16 Revision C.01, Gaussian Inc., Wallingford, CT (2016).
- [32] P. J. Stephens, F. J. Devlin, C. F. Chabalowski, and M. J. Frisch, *J. Phys. Chem.* **98**, 11623 (1994).
- [33] R. A. Kendall, T. H. Dunning, Jr., and R. J. Harrison, *J. Chem. Phys.* **96**, 6796 (1992).
- [34] U. Hergenhahn, O. Kugeler, A. Rüdél, E. E. Rennie, and A. M. Bradshaw, *J. Phys. Chem. A* **105**, 5704 (2001).
- [35] D. Rolles, M. Braune, S. Cvejanović, O. Geßner, R. Hentges, S. Korica, B. Langer, T. Lischke, G. Prümper, A. Reinköster *et al.*, *Nature (London)* **437**, 711 (2005).

- [36] E. N. Lassette, *J. Chem. Phys.* **43**, 4479 (1965).
- [37] L.-H. Wang, X.-J. Du, Y.-C. Xu, Z.-W. Nie, D.-H. Wang, S.-X. Wang, and L.-F. Zhu, *J. Phys. Chem. A* **126**, 453 (2022).
- [38] X. Kang, L. Q. Xu, Y. W. Liu, S. X. Wang, K. Yang, Y. G. Peng, D. D. Ni, N. Hiraoka, K. D. Tsuei, and L. F. Zhu, *J. Phys. B: At., Mol. Opt. Phys.* **52**, 245202 (2019).
- [39] R. B. Kay, P. E. Van der Leeuw, and M. J. Van der Wiel, *J. Phys. B: At. Mol. Phys.* **10**, 2513 (1977).
- [40] A. Bianconi, H. Petersen, F. C. Brown, and R. Z. Bachrach, *Phys. Rev. A* **17**, 1907 (1978).
- [41] J. L. Dehmer and D. Dill, *J. Chem. Phys.* **65**, 5327 (1976).
- [42] T. N. Rescigno and P. W. Langhoff, *Chem. Phys. Lett.* **51**, 65 (1977).
- [43] S. Iwata, N. Kosugi, and O. Nomura, *Jpn. J. Appl. Phys.* **17**, 109 (1978).
- [44] A. Barth and J. Schirmer, *J. Phys. B: At. Mol. Phys.* **18**, 867 (1985).
- [45] W. M. Kosman and S. Wallace, *J. Chem. Phys.* **82**, 1385 (1985).
- [46] A. Kalinko, W. A. Caliebe, R. Schoch, and M. Bauer, *J. Synchrotron Radiat.* **27**, 31 (2020).
- [47] P. Glatzel, A. Harris, P. Marion, M. Sikora, T.-C. Weng, C. Guilloud, S. Lafuerza, M. Rovezzi, B. Detlefs, and L. Ducotté, *J. Synchrotron Radiat.* **28**, 362 (2021).